applied sciences

MDPI

Article

Reduced Homogeneous Myocardial [^{18}F]FDG Uptake in Routine PET/CT Studies as an Early Indicator of Chemotherapy-Induced Cardiotoxicity

David Palomino-Fernández [1], Héctor Bueno [2,3,4,5], Carmen Jiménez-López-Guarch [2,3,4], Guillermo Moreno [3,6], Alexander P. Seiffert [1,7], Enrique J. Gómez [1,7,8], Adolfo Gómez-Grande [2,9] and Patricia Sánchez-González [1,7,8,*]

1 Biomedical Engineering and Telemedicine Centre, ETSI Telecomunicación, Center for Biomedical Technology, Universidad Politécnica de Madrid, 28040 Madrid, Spain; david.palomino.fernandez@alumnos.upm.es (D.P.-F.); ap.seiffert@upm.es (A.P.S.); enriquejavier.gomez@upm.es (E.J.G.)
2 Facultad de Medicina, Universidad Complutense de Madrid, 28040 Madrid, Spain; hector.bueno@cnic.es (H.B.); cjlguarch@gmail.com (C.J.-L.-G.); adolfo.gomez@salud.madrid.org (A.G.-G.)
3 Cardiology Department, Instituto de Investigación Sanitaria (imas12), Hospital Universitario 12 de Octubre, 28041 Madrid, Spain; guimoren@ucm.es
4 Centro de Investigación Biomédica en Red de enfermedades Cardiovasculares (CIBERCV), 28029 Madrid, Spain
5 Centro Nacional de Investigaciones Cardiovasculares (CNIC), 28029 Madrid, Spain
6 Facultad de Enfermería, Fisioterapia y Podología, Universidad Complutense de Madrid, 28040 Madrid, Spain
7 Instituto de Investigación Hospital 12 de Octubre (imas12), Hospital Universitario 12 de Octubre, 28041 Madrid, Spain
8 Centro de Investigación Biomédica en Red de Bioingeniería, Biomateriales y Nanomedicina, Instituto de Salud Carlos III, 28029 Madrid, Spain
9 Department of Nuclear Medicine, Hospital Universitario 12 de Octubre, 28041 Madrid, Spain
* Correspondence: p.sanchez@upm.es

Abstract: Cardiotoxicity refers to the damage induced by antineoplastic treatments, leading to various cardiovascular conditions. [^{18}F]FDG PET radiomics analysis could provide relevant information on early onset changes occurring in cardiac metabolism of chemotherapy-induced cardiotoxicity. Patients' sociodemographic data, cardiovascular risk factors, laboratory parameters, and left ventricle [^{18}F]FDG PET radiomic features are analyzed. The H_{Rad} index for the quantification of the heterogeneity of the metabolic uptake patterns is proposed. Statistical analysis is performed by separating patients according to the diagnosis of cancer therapy-related cardiac dysfunction (CTRCD). Baseline, intermediate, and end-of-treatment scans are evaluated as separate groups. Overall, CTRCD+ patients show lower overall mean standardized uptake values (SUV_{mean}) compared to CTRCD− patients, with statistically significant differences between groups only observed in the intermediate PET study (p = 0.025). A total of 34 radiomic features show statistically significant differences between the CTRCD+ and CTRCD− groups in the intermediate imaging studies. In the CTRCD− group, greater overall heterogeneity of metabolic uptake is observed in the intermediate PET image compared to the CTRCD+ groups (p = 0.025). The assessment of CTRCD through [^{18}F]FDG PET radiomics analysis could be a potential tool for the identification of a predisposition to the later development of cardiac complications after cardiotoxic treatment.

Keywords: [^{18}F]FDG PET; myocardial metabolism; cardiotoxicity; cancer therapy-related cardiac dysfunction; radiomics; early diagnosis

check for updates

Citation: Palomino-Fernández, D.; Bueno, H.; Jiménez-López-Guarch, C.; Moreno, G.; Seiffert, A.P.; Gómez, E.J.; Gómez-Grande, A.; Sánchez-González, P. Reduced Homogeneous Myocardial [^{18}F]FDG Uptake in Routine PET/CT Studies as an Early Indicator of Chemotherapy-Induced Cardiotoxicity. *Appl. Sci.* **2024**, *14*, 11653. https://doi.org/10.3390/app142411653

Academic Editor: Francesca Silvagno

Received: 12 November 2024
Revised: 11 December 2024
Accepted: 12 December 2024
Published: 13 December 2024

Copyright: © 2024 by the authors. Licensee MDPI, Basel, Switzerland. This article is an open access article distributed under the terms and conditions of the Creative Commons Attribution (CC BY) license (https://creativecommons.org/licenses/by/4.0/).

1. Introduction

The efficacy of antineoplastic treatments has increased with a resulting decrease in mortality in cancer patients in recent years [1]. However, some therapeutic schemes employ

cardiotoxic drugs that can cause cardiac damage or other cardiovascular alterations and are responsible for increased morbidity and mortality in cancer survivors [2–7]. Since the occurrence of cardiotoxicity is associated with poor prognosis [3,5], identifying it at an early subclinical stage is of vital importance to prevent it, establish cardioprotective treatments, and/or change chemotherapy schemes. Strategies for early detection of cardiotoxicity have been recently proposed in clinical cardio-oncology guidelines endorsed by the European Society of Cardiology [8] and include adequate risk stratification, the detection of abnormal serum biomarkers, such as troponin of natriuretic peptides, or performing cardiac imaging techniques [2–4], such as echocardiography or cardiac magnetic resonance (CMR). Given its safety, availability, reproducibility, and low cost, 2D ultrasound is the first-line method for the assessment of ventricular function changes, heart failure risk stratification, and treatment management [8]. However, other advanced imaging techniques, including 3D echocardiography [9], assessing myocardial deformation (global longitudinal strain) [10–12], or tissue characterization with CMR are now available to increase the sensitivity for the diagnosis of subtle myocardial damage [3,4].

The current clinical procedures are designed to detect cardiotoxicity when myocardial damage has already been established, not before. In this context, the use of positron emission tomography/computed tomography (PET/CT) studies with [^{18}F]fluorodeoxyglucose ([^{18}F]FDG) in oncological patients is now widely used both for the diagnosis and assessment of treatment response and follow-up. In recent years, and despite the difficult interpretation, different findings using [^{18}F]FDG PET have been proposed as potentially useful for early identification of cardiotoxicity, including uptake levels [13–16] or uptake patterns [17–19]. However, most of these studies lack standardized segmentation and quantification methods or a study population with echocardiography confirmed by cardiotoxicity diagnosis or even a control group. Therefore, baseline and follow-up oncologic [^{18}F]FDG PET images are not used for the early identification of abnormalities in myocardial metabolism in current routine clinical practice.

Furthermore, the changes in cardiac metabolism that suggest cardiotoxicity are not well established yet. Whereas previous research has suggested that an increased myocardial uptake occurs due to the effect of chemotherapy [13–16,19–24], it appears that decreased uptake may be more specific of myocardial damage [25]. New measurement tools, such as radiomic-based quantification methods [26–31] integrated into the analysis of [^{18}F]FDG PET/CT, may provide insight into the early changes occurring in cardiac metabolism associated with cardiotoxicity and would allow the implementation of personalized therapies aimed at preventing the deterioration of cardiac function.

The present study aims to describe the changes in myocardial metabolic uptake observed in patients with cancer treated with chemotherapy who undergo routine [^{18}F]FDG PET/CT imaging and explore the relationship between changes in FDG uptake radiomic patterns and the development of chemotherapy-induced cardiotoxicity.

2. Materials and Methods

The present study is a retrospective cohort study including all patients with echocardiographic findings consistent with cardiotoxicity who underwent whole body [^{18}F]FDG PET/CT imaging before, during, and after chemotherapy with a retrospective quantitative evaluation of all available cardiac uptakes.

2.1. Patients

We retrospectively identified all patients with a diagnosis of solid or hematologic cancer, who received chemotherapy with potential treatment-related cardiovascular toxicity and had at least one [^{18}F]FDG PET/CT scan performed between the years 2014 and 2022 at Hospital Universitario 12 de Octubre, Madrid, Spain. We selected those patients who also fulfilled the following criteria: (1) no known structural heart disease at the time of cancer diagnosis (this encompasses non-coronary cardiac disease processes, including heart valve disease, cardiomyopathy, and congenital heart disease [32]), (2) an available echocardio-

gram performed after concluding the potential cardiotoxic chemotherapy regimen, and (3) the presence of myocardial uptake in [^{18}F]FDG PET/CT scans performed before the chemotherapy regimen [33]. A diagnosis of moderate to severe cancer therapy-related cardiac dysfunction (CTRCD) was defined by means of an echocardiographic-derived left ventricular ejection fraction (LVEF) <50%. The presence of symptoms, elevated serum biomarkers, or echocardiographic-derived global longitudinal strain reduction alone was not considered for the definition of CTRCD [8,34]. All patients had received a chemotherapy regimen with potential cardiotoxicity previous to the intermediate [^{18}F]FDG PET/CT scans, to ensure a plausible cardiotoxicity timeline. The exclusion criteria included (1) suppressed myocardial uptake in all studies, (2) chemotherapy regimen not including cardiotoxic drugs, and (3) diagnosis of myocarditis or other forms of cancer therapy-related cardiovascular toxicity besides CTRCD during follow-up. Patients were considered CTRCD+ if the documented LVEF was below 50% and CTRCD− if the echocardiogram showed normal LVEF.

Patients' sociodemographic data and classic cardiovascular risk factors (sex, smoking, age, diabetes, hypertension, dyslipidemia) were collected and analyzed. The presence of radiotherapeutic treatment was also reported. The presence of any cardiovascular comorbidities other than structural heart disease (such as atrial fibrillation) was also documented, along with cardiovascular risk factors, which were summarized in a variable designated as cardiovascular history. Baseline demographic data, cardiovascular risk factors (hypertension, diabetes, dyslipidemia, smoking), and the presence of comorbidities were collected in all patients prior to the baseline image study.

Additionally, laboratory parameters were collected for baseline, intermediate, and EOT image studies. The laboratory test conducted nearest in time to each imaging study was chosen for analysis. The laboratory parameters collected were hemoglobin, red blood cells, hematocrit, mean corpuscular volume (MCV), mean corpuscular hemoglobin (MCH), mean corpuscular hemoglobin concentration (MCHC), leukocytes, neutrophils (% and $\times 10^3/mm^3$), lymphocytes (% and $\times 10^3/mm^3$), monocytes (% and $\times 10^3/mm^3$), eosinophils (% and $\times 10^3/mm^3$), basophils (% and $\times 10^3/mm^3$), platelets, mean platelet volume (MPV), glucose, total cholesterol, HDL cholesterol, LDL cholesterol, lipoprotein A (LpA), creatinine, glomerular filtrate (ckd-epi), troponin T (Tnt), calcium, potassium, sodium, chlorine, gamma-GT, total and direct bilirubin, alanine aminotransferase (ALT/GPT), aspartate aminotransferase (AST/GOT), gamma-glutamyl transferase (GGT), alkaline phosphatase (ALP), NT-proBNP, TSH, ferritin, total proteins, C-reactive protein, and erythrocyte sedimentation rate (ESR).

2.2. Image Acquisition

The detailed description of image acquisition settings, previously defined in [33], are presented in Supplementary Table S1. In brief, all patients undergo a minimum of a 6-h fasting period prior to the administration of the radiotracer. Two different scanners were employed for image acquisition (Siemens Biograph 6 True Point, Siemens Healthineers AG, Erlangen, Germany, and GE Discovery MI, GE HealthCare, Chicago, IL, USA). [^{18}F]FDG was administered intravenously at an average dose of 5 MBq/kg and 3 MBq/kg for the Siemens and GE scanners, respectively. The decision to use different doses was made by comparing the images and SUVs acquired on both imaging equipment to avoid much deviation with tumor response assessment when acquired on different equipment. Attenuation correction was performed via a low-dose CT scan.

2.3. Image Processing

All images were processed using the software CASSIA version 2.0 developed by our group [35]. The comprehensive [^{18}F]FDG PET/CT image processing methods utilized for the quantification of the myocardial metabolic activity was detailed in previous work [33]. Briefly, imaging data must be preprocessed prior to feature extraction following Image Biomarker Standardisation Initiative (IBSI) recommendations [36]. Volume of interest (VOI)

segmentation of the left ventricle [^{18}F]FDG metabolic activity, gray level discretization, and radiomic feature extraction were computed prior to radiomic data analysis. A standardized uptake value (SUV) was considered to quantize the PET images and compute the radiomic parameters. The segmentation of the metabolically active left ventricle volume in the PET image is conducted by thresholding (determining an optimal reference threshold within the left ventricular cavity for the segmentation of the left ventricle active metabolic volume [37]).

Radiomic features were extracted from the metabolically active left ventricle volume in the original non-filtered [^{18}F]FDG PET images by means of the open-source Python version 3.6.2 package Pyradiomics [38] with the default parameters, except resampledPixelSpacing set to $1 \times 1 \times 1$ mm^3; binWidth set to 0.125 SUV; resegmentMode set to absolute; and resegmentRange set to [0, 40.94] SUV (according to the SUV range of the study population). The radiomic feature extraction with the specified parameter configuration yielded a total of 94 image-based features: 19 First Order Statistics, 24 Gray Level Co-occurrence Matrix (GLCM), 16 Gray Level Run Length Matrix (GLRLM), 16 Gray Level Size Zone Matrix (GLSZM), 5 Neighboring Gray Tone Difference Matrix (NGTDM), and 14 Gray Level Dependence Matrix (GLDM). The comprehensive description of each radiomic feature, in compliance with the IBSI [36], can be accessed in the Pyradiomics documentation available at the Pyradiomics website (https://pyradiomics.readthedocs.io/en/latest/, accessed on 11 November 2024).

Lastly, the H_{Rad} index for the quantification of the heterogeneity of the metabolic uptake patterns is proposed. According to the definitions provided by the IBSI [36], the radiomic variables were assigned a contribution coefficient (C_i) whether they relate to the heterogeneity ($C_i = 1$) or homogeneity ($C_i = -1$) of the distribution of pixel intensities, or if they do not describe heterogeneity or homogeneity at all ($C_i = 0$). The specific contribution coefficients assigned to each feature can be found in Supplementary Table S2. Therefore, the H_{Rad} index is computed as follows:

$$H_{Rad} = \sum_{i=0}^{N} C_i \times F_i, \quad (1)$$

with N being the number of extracted radiomic features, F_i the value of the radiomic feature, and C_i the specific contribution coefficient defined for that feature according to the definitions provided by the IBSI [36].

2.4. Statistical Analysis

Patients were separated into CTRCD+ and CTRCD− groups. Therefore, statistical analysis was performed comparing both groups. Baseline, intermediate, and end-of-treatment (EOT) scans were treated as separate study subgroups. Continuous variables are represented as mean ± standard deviation. Differences in continuous variables were studied by means of the Mann–Whitney U-test and Benjamini Hochberg correction procedure for multiple comparison (only p-values < 0.05 after Benjamini Hochberg correction were retained). Differences over time between baseline, intermediate, and EOT studies were studied by means of the Kruskal–Wallis test with post-hoc analyses, where applicable (p-values < 0.05 were eligible for post-hoc analysis). Differences in categorical variables were studied with Chi-squared test. Statistical analyses were performed in SPSS software version 19.00 (IBM Corp., Armonk, NY, USA). Radiomic features with an intraclass correlation coefficient (ICC) above 0.82 that were identified in a previous study [33] were defined as robust indices and included in the analysis. This threshold was set at the midpoint of the range interval [0.75–0.90] revealing good feature robustness [39,40] with respect to variations in voxel size and gray level discretization.

A kNN model-based imputer (1-NN) was utilized to impute the missing values by means of the Orange 3.31 software (Bioinformatics Laboratory at the University of Ljubljana, Slovenia; https://orangedatamining.com/, accessed on 11 November 2024). A decision was made to remove the features with more than 10 instances exhibiting missing values.

2.5. Ethics

The study was approved by the Ethics Committee for Clinical Research (internal code 23/369, approved on 25 July 2023) and was carried out in accordance with the ethical principles of the Helsinki Declaration and the Basic Law of Data Protection (Data Protection Act 15/1999). Baseline, intermediate, and EOT [^{18}F]FDG PET/CT images were retrospectively collected.

3. Results

3.1. Patients and Demographic Features

Between January 2014 and December 2022, we identified 29 patients who fulfilled the inclusion criteria previously referred (baseline characteristics in Supplementary Tables S3 and S4) at a mean time after the initiation of potential cardiotoxic chemotherapy of 29.7 ± 40.5 months. The remaining 14 patients had at least one echocardiogram performed after the chemotherapy regime showing no structural abnormalities and normal LVEF.

The baseline features of the 29 patients included are presented in Supplementary Table S3, and the comparison between CTRCD groups in Supplementary Table S4. Mean age of participants was 51 ± 17 years, 17 (58.6%) women. All participants received a potentially cardiotoxic treatment; 93.1% with anthracyclines, ABVD (adriamycin, bleomycin sulfate, vinblastine sulfate, dacarbazine), R-CHOP (rituximab, cyclophosphamid, hydroxydaunorubicin, oncovin, prednisone), or doxorubicin. One patient received chemotherapy (platinum-based) combined with immunotherapy, and one patient received a combination of anthracyclines and immunotherapy. Radiotherapy was part of the treatment for five patients (17.2%) with a median dose of 30 Gy (range: 18–44 Gy), and of these, only two patients (6.9%) received radiotherapy targeting the left hemithorax. Compared with patients without cardiotoxicity, those with criteria consistent with cardiotoxicity were 12 years older (p = 0.05) on average but with no statistically significant differences in baseline characteristics.

3.2. Laboratory Parameters

After missing data imputation, HDL cholesterol, LDL cholesterol, LpA, ckd-epi, Tnt, NT-proBNP, and ESR were not included in the analysis (over 10 instances of missing values).

The remaining laboratory test parameters presenting statistically significant differences between CTRCD− vs. CTRCD+ groups were identified in baseline (Supplementary Table S5), intermediate (Supplementary Table S6), and EOT (Supplementary Table S7) studies. Ferritin (CTRCD+: 747 ± 499.11 vs. CTRCD−: 272.93 ± 365.77; p = 0.021; Supplementary Figure S1), hematocrit (CTRCD+: 31.11 ± 4.93 vs. CTRCD−: 37.04 ± 3.04; p = 0.015; Supplementary Figure S2), hemoglobin (CTRCD+: 3.52 ± 0.81 vs. CTRCD−: 4.30 ± 0.45; p = 0.030; Supplementary Figure S3), and red blood cells (CTRCD+: 10.33 ± 1.62 vs. CTRCD−: 12.38 ± 1.02; p = 0.006; Supplementary Figure S4) showed statistically significant differences after multiple testing correction between CTRCD+ and CTRCD− groups in the intermediate studies, with the latter three exhibiting lower values in the CTRCD+ group. No features remained statistically significant after multiple testing correction in baseline and EOT studies.

Differences between baseline, intermediate, and EOT laboratory parameters were studied within each CTRCD+ and CTRCD− groups separately, as shown in Supplementary Table S8 and Supplementary Table S9, respectively. CTRCD+ showed changes over time in AST/GOT (p = 0.018) and monocytes (p = 0.044) values between baseline, interim, and EOT imaging studies (Supplementary Table S8). However, the differences were not statistically significant after multiple testing correction. CTRCD− showed changes over time in red blood cells (p = 0.001) and monocytes (p = 0.000) values between baseline, interim, and EOT imaging studies (Supplementary Table S9). Red blood cells and monocytes differences over time remained statistically significant after multiple testing correction and post-hoc analysis were conducted. Specifically, the CTRCD− group exhibited an overall decrease in red blood cells levels between baseline and intermediate (CTRCD− [baseline]: 4.90 ± 0.56 vs.

CTRCD− [intermediate]: 4.30 ± 0.45, $p = 0.007$) and baseline and EOT studies (CTRCD− [baseline]: 4.90 ± 0.56 vs. CTRCD− [EOT]: 4.19 ± 0.45, $p = 0.001$), as shown in Supplementary Figure S4. Moreover, an overall increase in monocytes levels between baseline and intermediate was observed in the CRTCD− group (CTRCD− [baseline]: 7.46 ± 3.59 vs. CTRCD− [intermediate]: 16.41 ± 10.81, $p = 0.001$) and baseline and EOT studies (CTRCD− [baseline]: 7.46 ± 3.59 vs. CTRCD− [EOT]: 12.79 ± 4.01, $p = 0.005$), as shown in Supplementary Figure S5.

3.3. Image-Based Features

Overall, CTRCD+ patients showed lower SUV_{max} values compared with CTRCD− patients (Figure 1a), both in the baseline, intermediate, and EOT imaging studies, with statistically significant differences in the SUV_{max} values between groups only present in the intermediate PET (CTRCD+: 8.28 ± 0.40 vs. CTRCD−: 15.26 ± 0.40, $p = 0.009$).

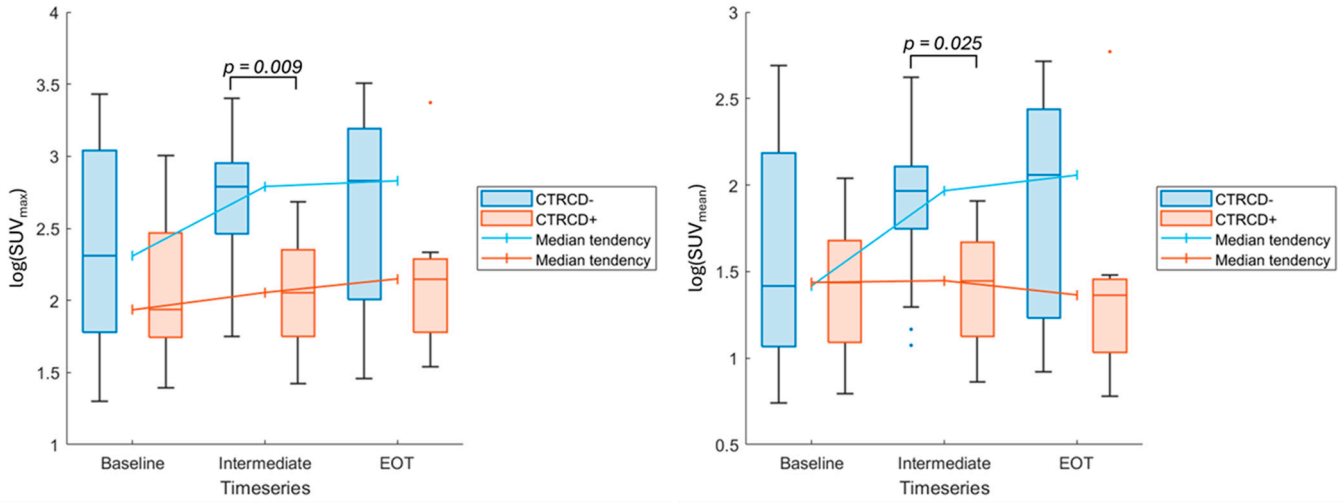

(**a**) (**b**)

Figure 1. Comparison of value distribution and change over time (baseline, intermediate, and EOT) in the mean [^{18}F]FDG PET/CT scan SUV values between the CTRCD+ and CTRCD− groups. The vertical axis is expressed in log scale to evidence the differences between groups. Statistically significant differences between CTRCD groups after multiple-testing correction are indicated with their respective *p*-values. (**a**) SUV_{max}. (**b**) SUV_{mean}. SUV: standardized uptake value; EOT: end-of-treatment.

Similarly, CTRCD+ patients showed lower overall SUV_{mean} values compared with CTRCD− patients (Figure 1b), with statistically significant differences in the SUV_{mean} values between groups only observed in the intermediate PET study (CTRCD+, 4.30 ± 0.32 vs. CTRCD−, 7.10 ± 0.39, $p = 0.025$).

Radiomic features were also obtained to assess the differences between CTRCD groups (Supplementary Table S10). A total of 34 radiomic features showed statistically significant differences between the CTRCD+ and CTRCD− groups in the intermediate image studies: 14 first-order features (including SUV_{max} and SUV_{mean}), 6 GLCM features, 4 GDLM features, 8 GLRLM features, and 2 GLSZM features. No statistically significant differences between CTRCD groups were observed in the radiomic features in baseline and EOT image studies.

The H_{Rad} index distribution is shown in Figure 2. In the CTRCD− group, an overall increased heterogeneity of the metabolic uptake in the intermediate PET image was observed compared to the CTRCD+ group. Statistically significant differences in the H_{Rad} index values were found in the intermediate PET between groups (CTRCD+: 7.15 ± 0.45 vs. CTRCD−: 13.18 ± 0.40, $p = 0.025$).

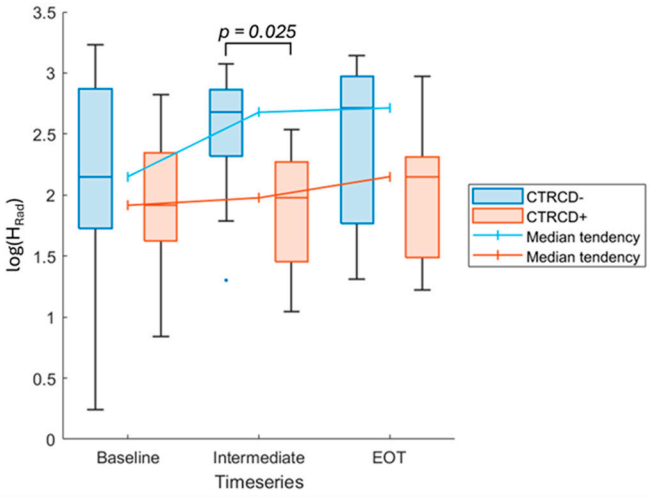

Figure 2. H_{Rad} index distribution and trends in median values for the CTRCD+ and CTRCD− groups in the baseline, intermediate, and EOT image studies. The vertical axis is expressed in log scale to evidence the differences between groups. Statistically significant differences between CTRCD groups after multiple-testing correction are indicated with their respective *p*-values. CTRCD: cancer therapy-related cardiac dysfunction; EOT: end-of-treatment.

4. Discussion

According to cardio-oncology recommendations, strategies for the early detection of cardiotoxicity include the use of biomarkers and cardiac imaging techniques [2–4] with a multidisciplinary approach [2,3,5], with protocols for the prevention and diagnosis of cardiotoxicity in patients with chemotherapy treatment recently defined [2–4,8,34,41,42].

The early diagnosis of myocardial damage derived from anthracycline treatment is a crucial factor for reducing the risk or consequences of cardiotoxicity. The quantification of routinely acquired oncological [^{18}F]FDG PET imaging studies may provide further insight into the early diagnosis of myocardial imparities, as stated in the literature [13–16,19–24]. The study of the intrinsic characteristics of the images through radiomics has also shown promising potential in the diagnosis of various cardiac diseases [26–31,43].

Our results show that of the patients with documented moderate to severe CTRCD+, most of them treated with anthracyclines have a significative decreased metabolic uptake in the intermediate [^{18}F]FDG PET study compared with the CTRCD− group. Moreover, to the best of our knowledge, this is the first study that analyzes the utility of radiomic [^{18}F]FDG/PET features in the follow-up of patients treated with potential cardiotoxic chemotherapy, showing significant differences in the intermediate PET study results between the groups with and without CTRCD.

The evidence regarding the use of [^{18}F]FDG PET imaging to detect cardiotoxicity at an early stage is still scarce, partly due to the variability in metabolic uptake [13–16,19–24]. Moreover, most studies defined exclusion criteria based on the presence of previous risk factors [13–16,22,23] and therefore do not study the potential predictive value of clinical variables in favor of more homogeneous cohorts. On the contrary, we considered cardiovascular risk factors in this study, findings a higher prevalence of HTN (p = 0.013) and older age (p = 0.005) in the CTRCD+ group. The cohort included five patients who received radiotherapy as part of their treatment. Among them, two patients (from the CRTCD− group) underwent radiotherapy involving the left hemithorax, while the remaining three patients (from the CRTCD+ group) received radiotherapy in areas distant from the left hemithorax, such as the pelvis. While radiotherapy is recognized as an integral component of the treatment strategy for these patients and may influence cardiac functionality, only three patients in the cohort received radiotherapy specifically targeting the left hemithorax. This limits the statistical evaluation of its correlation with altered metabolic uptake patterns.

Given the routine use of [^{18}F]FDG PET during many oncology treatments, the potential changes in myocardial [^{18}F]FDG uptake became an attractive biomarker in the early detection of cardiotoxicity. This has been evaluated using different approaches, including dose-dependent uptake increase for Adriamycin [13,21] or doxorubicin-induced [14] cardiotoxicity, focal uptake increase in the right [23] or left ventricle [19,20,22] in PET studies performed while on treatment, and myocardial uptake patterns in follow-up PET studies revealing reduced uptake at baseline [14] and increased uptake in intermediate [19,33] or post-treatment studies [16,23] in the patients with a higher incidence of cardiac abnormalities. Overall, previous studies described increased myocardial metabolic activity associated with the cardiotoxic effects of chemotherapy [13–16,19–24] but with marked differences between them. The first subset of studies described an increase in [^{18}F]FDG PET myocardial uptake following cardiotoxic treatments [13,20–22]. However, follow-up studies proposed further patterns of myocardial uptake related to the potential development of CTRCD [14–16,19,23,24]. In fact, most of these studies show an effect of anthracyclines in the treated population without specifying whether cardiotoxicity developed during or after the treatment. In our series, we found a lack of overall increase in [^{18}F]FDG myocardial uptake during treatment in the CTRCD+ group compared with the CTRCD− group.

Becker et al. [25] suggested that cardiomyocytes may exhibit a potential vulnerability to oxidative damage, mainly related to a lower baseline level of antioxidant enzymes and elevated mitochondria concentration. Indeed, previous research has pointed to the reactive oxygen species as the most accepted mechanism involved in the development of cardiotoxicity [44]. The oxidative stress may eventually lead to structural and functional damage to the cardiomyocytes, and consequently, a reduction in the [^{18}F]FDG uptake in the affected myocardium should be expected [25]. Although initial studies reported an increased uptake of [^{18}F]FDG in the myocardium of patients undergoing chemotherapy [14,16,23], these did not include patients with cardiovascular risk factors, whose myocardium could respond differently due to a greater vulnerability to the damage produced by anthracyclines [45]. Moreover, consistent with the hypothesis of oxidative damage and a potential reduction in the capacity of vulnerable myocardium to be responsive to cardiotoxic damage, our results reveal that CTRCD+ patients showed significantly lower uptake values compared to CTRCD− patients during the intermediate PET imaging studies. Nonetheless, it is important to mention that the mechanisms of cardiotoxicity and glycolytic metabolism in exposed cardiomyocytes have not yet been well established and are mere hypotheses.

Similarly, methodologies for the quantification of cardiac metabolism in nuclear imaging are not yet standardized or well-established yet. As a rule, the quantification of cardiac [^{18}F]FDG PET activity is performed based on region/volume of interest manually placed on cardiac structures that show measurable focal uptake. Nevertheless, the assessment of cardiac FDG uptake patterns could benefit from more sophisticated analyses such as radiomic-based quantification methods. Previous studies [26–31] have shown a potential diagnostic role of radiomic features in various cardiac diseases, such as texture analysis in patients with cardiac sarcoidosis [26,31], heart failure-like myocarditis [28] or acute infarct-like myocarditis [29], and prediction of long-term outcome in patients with takotsubo syndrome [30].

To the best of our knowledge, this is the first study to extend the concept of the analysis of [^{18}F]FDG PET radiomics to the assessment of cardiac toxicity with routine follow-up scans. A total of 34 radiomic features were identified as potential predictors of cardiotoxicity in the intermediate PET study, which could be a potential tool to support the identification of a predisposition to the subsequent development of cardiac complications after cardiotoxic treatment or the early diagnosis, which would allow for improvement in the clinical management of these patients through the use of other treatment strategies that preserve myocardial functionality. The H_{Rad} uptake heterogeneity index based on the radiomic values revealed that the myocardium of CTRCD+ patients exhibited greater homogeneity in [^{18}F]FDG uptake in the intermediate PET studies combined with lower overall uptake in the intermediate PET associated with cardiotoxic damage ($p = 0.025$). Therefore, [^{18}F]FDG

PET homogeneous uptake patterns may be a marker of initial myocardial damage compared with the heterogeneity found in healthy myocardium during follow-up studies becoming a potential radiomic predictor of cardiotoxicity.

Although no other studies have described texture patterns related to cardiotoxic damage so far, previous research works associated increased texture heterogeneity with poorer prognosis and response to treatment in patients with Hodgkin lymphoma [27] or cardiovascular conditions such as myocarditis [28,29]. Yet, some studies have also suggested greater homogeneity and a higher prevalence of high uptake intensities in cardiovascular disorders such as cardiac sarcoidosis [26,31]. Nevertheless, our results demonstrate, through the identified radiomic predictors, the association between texture homogeneity and lower uptake patterns in the CTRCD+ group. Some first-order features such as entropy or uniformity support this hypothesis. Entropy specifies the uncertainty/randomness of the image values, with higher values associated with CTRCD−, i.e., higher heterogeneity. Uniformity is a measure of the sum of squares of each intensity value. It is a measure of the homogeneity of the image, with higher values associated with CTRCD+. Higher order radiomic features provide information about the textures in myocardial uptake. Consistent with the suggested hypothesis, these features evidence a more homogeneous texture for CTRCD+, based on the similarity of pixels from neighboring areas. For example, the GLRLM RunPercentage feature measures the coarseness of the texture, with higher values associated with CTRCD−, indicating a greater presence of small groups of pixels with similar intensities (indicating a finer texture, i.e., greater heterogeneity). Similarly, the GLRLM RunLengthNonUniformity feature measures the variability in gray level intensity values in the image; a lower value indicates more homogeneity in intensity values and is associated with CTRCD+. Additionally, some texture features such as GLRLM ShortRunLowGrayLevelEmphasis measure the joint distribution of smaller similarity zones and lower intensity levels, with greater values associated with CTRCD+. In general, texture features demonstrate lower intensity values in myocardial uptake in CTRCD+.

Regarding the laboratory test parameters, significant differences were identified between the CTRCD− and CTRCD+ groups at different stages of the study. Statistically significant differences were observed in the intermediate studies for ferritin, hematocrit, hemoglobin, and red blood cells, with the CTRCD+ group exhibiting lower values for the latter three. Notably, red blood cells and monocytes exhibited significant changes over time within the CTRCD− group. Specifically, red blood cells decreased and monocytes increased from baseline to EOT, even after multiple testing correction. The observed differences at the intermediate stage indicate the potential impact of antineoplastic treatments on hematological parameters and processes. They may also reflect the cardiovascular toxicity effects of these treatments. The results indicate that monitoring certain drug parameters may be crucial for patients undergoing treatment that may lead to cardiac toxicity.

This study has methodological limitations, such as the retrospective nature of the study, the small single center-based study cohort, and the rough definition of cardiotoxicity. Some variables such as diet, which is known to affect the myocardial glucose uptake, could not be controlled. One of the main goals of future studies should be to assess the validity of the quantitative and radiomic features for the early diagnosis of cardiotoxicity-derived metabolic disorders prospectively in a larger patient cohort with standardized imaging and diet protocols.

Nevertheless, these findings could lead to a widespread multipurpose use of the [^{18}F]FDG/PET scans, providing a one-stop shop diagnostic tool both for cancer treatment efficacy and cardiac-related cardiotoxicity, thus guiding a closer monitoring of cardiac dysfunction and early indication of cardioprotective treatment. If the decrease in cardiac uptake is adequately validated through future prospective studies, potential changes in clinical practice and the management of these patients could be considered. For instance, tailored follow-up programs could be implemented, such as specific ultrasound or MRI studies for patients who routinely show reduced cardiac uptake on PET scans. In cases with a favorable response, dose de-escalation or treatment discontinuation could be considered,

while in others, switching to second-line therapies or implementing more rigorous control measures for cardiovascular risk factors might be necessary.

5. Conclusions

Routine [^{18}F]FDG PET studies performed during chemotherapy may be useful to detect cardiotoxicity at an early stage. Myocardial uptake values and patterns and some radiomic variables may predict myocardial damage produced by chemotherapy and help select patients who may benefit from other therapeutic options. Further research in this field is warranted and larger prospective patient cohorts should be evaluated.

Supplementary Materials: The following supporting information can be downloaded at https://www.mdpi.com/article/10.3390/app142411653/s1: Figure S1: Ferritin distribution and trends in median values for the CTRCD+ and CTRCD− groups in the baseline, intermediate, and EOT image studies. The vertical axis is expressed in log scale to evidence the differences between groups. Statistically significant differences between time series groups after multiple-testing correction are indicated with their respective *p*-values. CTRCD: cancer therapy-related cardiac dysfunction; EOT: end-of-treatment; Figure S2: Hematocrit distribution and trends in median values for the CTRCD+ and CTRCD− groups in the baseline, intermediate, and EOT image studies. The vertical axis is expressed in log scale to evidence the differences between groups. Statistically significant differences between time series groups after multiple-testing correction are indicated with their respective *p*-values. CTRCD: cancer therapy-related cardiac dysfunction; EOT: end-of-treatment; Figure S3: Hemoglobin distribution and trends in median values for the CTRCD+ and CTRCD− groups in the baseline, intermediate, and EOT image studies. The vertical axis is expressed in log scale to evidence the differences between groups. Statistically significant differences between time series groups after multiple-testing correction are indicated with their respective *p*-values. CTRCD: cancer therapy-related cardiac dysfunction; EOT: end-of-treatment. Figure S4: Red blood cell distribution and trends in median values for the CTRCD+ and CTRCD− groups in the baseline, intermediate, and EOT image studies. The vertical axis is expressed in log scale to evidence the differences between groups. Statistically significant differences between time series groups after multiple-testing correction and post-hoc analysis are indicated with their respective *p*-values. CTRCD: cancer therapy-related cardiac dysfunction; EOT: end-of-treatment; Figure S5: Monocyte distribution and trends in median values for the CTRCD+ and CTRCD− groups in the baseline, intermediate, and EOT image studies. The vertical axis is expressed in log scale to evidence the differences between groups. Statistically significant differences between time series groups after multiple-testing correction and post-hoc analysis are indicated with their respective *p*-values. CTRCD: cancer therapy-related cardiac dysfunction; EOT: end-of-treatment. Table S1: Imaging protocol. Adapted from [33]; Table S2: According to the definitions provided by the IBSI [36], the radiomic variables were assigned a contribution coefficient (C_i) whether they relate to the heterogeneity ($C_i = 1$) or homogeneity ($C_i = -1$) of the distribution of pixel intensities, or if they do not describe heterogeneity or homogeneity at all ($C_i = 0$) in order to compute the H_{Rad} index; Table S3: Patient demographics and baseline characteristics; Table S4: Baseline characteristics by cardiotoxicity group; Table S5: Laboratory test features presenting statistically significant differences between CTRCD− vs. CTRCD+ groups in baseline studies. No statistically significant features remained after multiple testing correction; Table S6: Laboratory parameters presenting statistically significant differences between CTRCD− vs. CTRCD+ groups in intermediate studies. *p*-values marked with * remained statistically significant after multiple testing correction; Table S7: Laboratory parameters presenting statistically significant differences between CTRCD− and CTRCD+ groups in EOT studies. No statistically significant features remained after multiple testing correction; Table S8: Laboratory parameters presenting statistically significant differences between baseline, intermediate, and EOT studies in the CTRCD+ group. No statistically significant features remained after multiple testing correction; Table S9: Laboratory parameters presenting statistically significant differences between baseline, intermediate, and EOT studies in the CTRCD− group. *p*-values marked with * remained statistically significant after multiple testing correction; Table S10: Radiomic and SUV features presenting statistically significant differences between CTRCD+ and CTRCD− groups after multiple-testing correction and were confirmed as robust radiomic indices (Consistency ICC > 0.82 for variations in gray level

discretization bin size) [33]. Only radiomic features obtained from intermediate image studies were retained. *p*-values marked with * remained statistically significant after multiple testing correction.

Author Contributions: Conceptualization: D.P.-F., H.B., C.J.-L.-G., G.M., A.P.S., E.J.G., A.G.-G. and P.S.-G.; Methodology: D.P.-F., H.B., A.P.S., A.G.-G. and P.S.-G.; Software: D.P.-F. and A.P.S.; Validation: D.P.-F., H.B., A.P.S., A.G.-G. and P.S.-G.; Formal analysis: D.P.-F. and A.P.S.; Investigation: D.P.-F., H.B., C.J.-L.-G., G.M., A.P.S., E.J.G., A.G.-G. and P.S.-G.; Resources: H.B., C.J.-L.-G., G.M., E.J.G., A.G.-G. and P.S.-G.; Data Curation: D.P.-F., C.J.-L.-G., G.M., A.G.-G. and A.P.S.; Writing—Original Draft Preparation: D.P.-F., C.J.-L.-G., A.P.S. and P.S.-G.; Writing—Review and Editing: D.P.-F., H.B., C.J.-L.-G., G.M., A.P.S., E.J.G., A.G.-G. and P.S.-G.; Visualization: D.P.-F., A.P.S. and P.S.-G.; Supervision: H.B. and P.S.-G. All authors have read and agreed to the published version of the manuscript.

Funding: The project was partially funded by a grant from the Sociedad Española de Cardiología (SEC/FEC-INV-BAS 22/023).

Institutional Review Board Statement: The study was conducted in accordance with the Declaration of Helsinki and approved by the Institutional Review Board (or Ethics Committee) of Hospital Universitario 12 de Octubre, Madrid, Spain (23/369, approved on 25 July 2023).

Informed Consent Statement: Informed consent was obtained from all subjects involved in the study.

Data Availability Statement: The original contributions presented in the study are included in the article\Supplementary Materials, further inquiries can be directed to the corresponding author.

Conflicts of Interest: Dr. Bueno receives research funding from the European Union (EU4H-2022-JA-03), Instituto de Salud Carlos III, Spain (PI21/01572), Sociedad Española de Cardiología, AstraZeneca, Boehringer Ingelheim, Janssen, and Novartis, and has received consulting/speaking fees from AstraZeneca, Novartis, Novo Nordisk and Organon. The other authors declare no conflicts of interest.

References

1. Miller, K.D.; Nogueira, L.; Mariotto, A.B.; Rowland, J.H.; Yabroff, K.R.; Alfano, C.M.; Jemal, A.; Kramer, J.L.; Siegel, R.L. Cancer Treatment and Survivorship Statistics, 2019. CA. *Cancer J. Clin.* **2019**, *69*, 363–385. [CrossRef]
2. Curigliano, G.; Lenihan, D.; Fradley, M.; Ganatra, S.; Barac, A.; Blaes, A.; Herrmann, J.; Porter, C.; Lyon, A.R.; Lancellotti, P.; et al. Management of Cardiac Disease in Cancer Patients throughout Oncological Treatment: ESMO Consensus Recommendations. *Ann. Oncol.* **2020**, *31*, 171–190. [CrossRef] [PubMed]
3. López-Fernández, T.; Martín García, A.; Santaballa Beltrán, A.; Montero Luis, Á.; García Sanz, R.; Mazón Ramos, P.; Velasco del Castillo, S.; López de Sá Areses, E.; Barreiro-Pérez, M.; Hinojar Baydes, R.; et al. Cardio-Onco-Hematology in Clinical Practice. Position Paper and Recommendations. *Rev. Española Cardiol.* **2017**, *70*, 474–486. [CrossRef]
4. Bhagat, A.; Kleinerman, E.S. Anthracycline-Induced Cardiotoxicity: Causes, Mechanisms, and Prevention. *Adv. Exp. Med. Biol.* **2020**, *1257*, 181–192. [CrossRef] [PubMed]
5. Herrmann, J. Adverse Cardiac Effects of Cancer Therapies: Cardiotoxicity and Arrhythmia. *Nat. Rev. Cardiol.* **2020**, *17*, 474–502. [CrossRef] [PubMed]
6. Curigliano, G.; Cardinale, D.; Dent, S.; Criscitiello, C.; Aseyev, O.; Lenihan, D.; Cipolla, C.M. Cardiotoxicity of Anticancer Treatments: Epidemiology, Detection, and Management. CA. *Cancer J. Clin.* **2016**, *66*, 309–325. [CrossRef] [PubMed]
7. Novo, G.; Nugara, C.; Fava, A.; Mantero, A.; Citro, R. Early Detection of Myocardial Damage: A Multimodality Approach. *J. Cardiovasc. Echogr.* **2020**, *30*, S4–S10. [CrossRef]
8. Lyon, A.R.; López-Fernánde, T.; Couch, L.S.; Asteggiano, R.; Aznar, M.C.; Bergler-Klei, J.; Boriani, G.; Cardinale, D.; Cordoba, R.; Cosyns, B.; et al. 2022 ESC Guidelines on Cardio-Oncology Developed in Collaboration with the European Hematology Association (EHA), the European Society for Therapeutic Radiology and Oncology (ESTRO) and the International Cardio-Oncology Society (IC-OS): Developed by the Task Force on Cardio-Oncology of the European Society of Cardiology (ESC). *Eur. Heart J.* **2022**, *43*, 4229–4361. [CrossRef] [PubMed]
9. Zito, C.; Longobardo, L.; Cadeddu, C.; Monte, I.; Novo, G.; Dell'oglio, S.; Pepe, A.; Madonna, R.; Tocchetti, C.G.; Mele, D. Cardiovascular Imaging in the Diagnosis and Monitoring of Cardiotoxicity: Role of Echocardiography. *J. Cardiovasc. Med.* **2016**, *17*, S45–S54. [CrossRef] [PubMed]
10. Sawaya, H.; Sebag, I.A.; Plana, J.C.; Januzzi, J.L.; Ky, B.; Tan, T.C.; Cohen, V.; Banchs, J.; Carver, J.R.; Wiegers, S.E.; et al. Assessment of Echocardiography and Biomarkers for the Extended Prediction of Cardiotoxicity in Patients Treated with Anthracyclines, Taxanes, and Trastuzumab. *Circ. Cardiovasc. Imaging* **2012**, *5*, 596–603. [CrossRef] [PubMed]
11. Oikonomou, E.K.; Kokkinidis, D.G.; Kampaktsis, P.N.; Amir, E.A.; Marwick, T.H.; Gupta, D.; Thavendiranathan, P. Assessment of Prognostic Value of Left Ventricular Global Longitudinal Strain for Early Prediction of Chemotherapy-Induced Cardiotoxicity: A Systematic Review and Meta-Analysis. *JAMA Cardiol.* **2019**, *4*, 1007–1018. [CrossRef] [PubMed]

12. Adamo, L.; Perry, A.; Novak, E.; Makan, M.; Lindman, B.R.; Mann, D.L. Abnormal Global Longitudinal Strain Predicts Future Deterioration of Left Ventricular Function in Heart Failure Patients with a Recovered Left Ventricular Ejection Fraction. *Circ. Heart Fail.* **2017**, *10*, e003788. [CrossRef] [PubMed]
13. Borde, C.; Kand, P.; Basu, S. Enhanced Myocardial Fluorodeoxyglucose Uptake Following Adriamycin-Based Therapy: Evidence of Early Chemotherapeutic Cardiotoxicity? *World J. Radiol.* **2012**, *4*, 220–223. [CrossRef]
14. Bauckneht, M.; Ferrarazzo, G.; Fiz, F.; Morbelli, S.; Sarocchi, M.; Pastorino, F.; Ghidella, A.; Pomposelli, E.; Miglino, M.; Ameri, P.; et al. Doxorubicin Effect on Myocardial Metabolism as a Prerequisite for Subsequent Development of Cardiac Toxicity: A Translational ^{18}F-FDG PET/CT Observation. *J. Nucl. Med.* **2017**, *58*, 1638–1645. [CrossRef] [PubMed]
15. Bauckneht, M.; Morbelli, S.; Fiz, F.; Ferrarazzo, G.; Piva, R.; Nieri, A.; Sarocchi, M.; Spallarossa, P.; Canepari, M.; Arboscello, E.; et al. A Score-Based Approach to ^{18}F-FDG PET Images as a Tool to Describe Metabolic Predictors of Myocardial Doxorubicin Susceptibility. *Diagnostics* **2017**, *7*, 57. [CrossRef] [PubMed]
16. Sarocchi, M.; Bauckneht, M.; Arboscello, E.; Capitanio, S.; Marini, C.; Morbelli, S.; Miglino, M.; Congiu, A.G.; Ghigliotti, G.; Balbi, M.; et al. An Increase in Myocardial 18-Fluorodeoxyglucose Uptake Is Associated with Left Ventricular Ejection Fraction Decline in Hodgkin Lymphoma Patients Treated with Anthracycline. *J. Transl. Med.* **2018**, *16*, 295. [CrossRef] [PubMed]
17. Gropler, R.J.; Siegel, B.A.; Lee, K.J.; Moerlein, S.M.; Perry, D.J.; Bergmann, S.R.; Geltman, E.M. Nonuniformity in Myocardial Accumulation of Fluorine-18-Fluorodeoxyglucose in Normal Fasted Humans. *J. Nucl. Med.* **1990**, *31*, 1749–1756. [PubMed]
18. Maurer, A.H.; Burshteyn, M.; Adler, L.P.; Steiner, R.M. How to Differentiate Benign versus Malignant Cardiac and Paracardiac ^{18}F FDG Uptake at Oncologic PET/CT. *Radiographics* **2011**, *31*, 1287–1305. [CrossRef] [PubMed]
19. Seiffert, A.P.; Gómez-Grande, A.; Castro-Leal, G.; Rodríguez, A.; Palomino-Fernández, D.; Gómez, E.J.; Sánchez-González, P.; Bueno, H. An Image Processing Tool for the Detection of Anthracycline-Induced Cardiotoxicity by Evaluating the Myocardial Metabolic Activity in [^{18}F]FDG PET/CT. *Int. J. Comput. Assist. Radiol. Surg.* **2022**, *17*, 373–383. [CrossRef] [PubMed]
20. Haider, A.; Bengs, S.; Schade, K.; Wijnen, W.J.; Portmann, A.; Etter, D.; Fröhlich, S.; Warnock, G.I.; Treyer, V.; Burger, I.A.; et al. Myocardial ^{18}F-FDG Uptake Pattern for Cardiovascular Risk Stratification in Patients Undergoing Oncologic PET/CT. *J. Clin. Med.* **2020**, *9*, 2279. [CrossRef] [PubMed]
21. Basu, S.; Borde, C.; Kand, P. Increasing Cardiac ^{18}F-Fluorodeoxyglucose (FDG) Uptake on PET–CT as a Biomarker for Cardiotoxicity of Chemo-Radiotherapy in Cancer: A Myth or a Reality? *Radiother. Oncol.* **2014**, *112*, 451–452. [CrossRef] [PubMed]
22. Ben Bouallègue, F.; Maïmoun, L.; Kucharczak, F.; Le Fur, P.; Vauchot, F.; Hay, B.; Rondet, E.; Mariano-Goulart, D. Left Ventricle Function Assessment Using Gated First-Pass ^{18}F-FDG PET: Validation against Equilibrium Radionuclide Angiography. *J. Nucl. Cardiol.* **2021**, *28*, 594–603. [CrossRef]
23. Kim, J.; Cho, S.G.; Kang, S.R.; Yoo, S.W.; Kwon, S.Y.; Min, J.J.; Bom, H.S.; Song, H.C. Association between FDG Uptake in the Right Ventricular Myocardium and Cancer Therapy-Induced Cardiotoxicity. *J. Nucl. Cardiol.* **2019**, *27*, 2154–2163. [CrossRef]
24. Bauckneht, M.; Cossu, V.; Miceli, A.; Donegani, M.I.; Capitanio, S.; Morbelli, S.; Marini, C.; Sambuceti, G. FDG-PET Imaging of Doxorubicin-Induced Cardiotoxicity: A New Window on an Old Problem. *Curr. Cardiovasc. Imaging Rep.* **2019**, *12*, 41. [CrossRef]
25. Becker, M.M.C.; Arruda, G.F.A.; Berenguer, D.R.F.; Buril, R.O.; Cardinale, D.; Brandão, S.C.S. Anthracycline Cardiotoxicity: Current Methods of Diagnosis and Possible Role of ^{18}F-FDG PET/CT as a New Biomarker. *Cardio-Oncology* **2023**, *9*, 17. [CrossRef] [PubMed]
26. Manabe, O.; Ohira, H.; Hirata, K.; Hayashi, S.; Naya, M.; Tsujino, I.; Aikawa, T.; Koyanagawa, K.; Oyama-Manabe, N.; Tomiyama, Y.; et al. Use of 18 F-FDG PET/CT Texture Analysis to Diagnose Cardiac Sarcoidosis. *Eur. J. Nucl. Med. Mol. Imaging* **2019**, *46*, 1240–1247. [CrossRef]
27. Reinert, C.P.; Wanek, L.; Bösmüller, H.; Federmann, B.; Fritz, J.; Sökler, M.; Horger, M. Computed Tomography Texture Analysis for Assessment of Chemotherapy Response of Hodgkin Lymphoma. *Medicine* **2020**, *99*, e19146. [CrossRef] [PubMed]
28. Baessler, B.; Luecke, C.; Lurz, J.; Klingel, K.; Das, A.; Von Roeder, M.; De Waha-Thiele, S.; Besler, C.; Rommel, K.P.; Maintz, D.; et al. Cardiac MRI and Texture Analysis of Myocardial T1 and T2 Maps in Myocarditis with Acute versus Chronic Symptoms of Heart Failure. *Radiology* **2019**, *292*, 608–617. [CrossRef]
29. Baessler, B.; Luecke, C.; Lurz, J.; Klingel, K.; Von Roeder, M.; De Waha, S.; Besler, C.; Maintz, D.; Gutberlet, M.; Thiele, H.; et al. Cardiac MRI Texture Analysis of T1 and T2 Maps in Patients with Infarctlike Acute Myocarditis. *Radiology* **2018**, *289*, 357–365. [CrossRef] [PubMed]
30. Mannil, M.; Kato, K.; Manka, R.; von Spiczak, J.; Peters, B.; Cammann, V.L.; Kaiser, C.; Osswald, S.; Nguyen, T.H.; Horowitz, J.D.; et al. Prognostic Value of Texture Analysis from Cardiac Magnetic Resonance Imaging in Patients with Takotsubo Syndrome: A Machine Learning Based Proof-of-Principle Approach. *Sci. Rep.* **2020**, *10*, 20537. [CrossRef]
31. Manabe, O.; Koyanagawa, K.; Hirata, K.; Oyama-Manabe, N.; Ohira, H.; Aikawa, T.; Furuya, S.; Naya, M.; Tsujino, I.; Tomiyama, Y.; et al. Prognostic Value of ^{18}F-FDG PET Using Texture Analysis in Cardiac Sarcoidosis. *JACC Cardiovasc. Imaging* **2020**, *13*, 1096–1097. [CrossRef]
32. Steinberg, D.H.; Staubach, S.; Franke, J.; Sievert, H. Defining Structural Heart Disease in the Adult Patient: Current Scope, Inherent Challenges and Future Directions. *Eur. Heart J. Suppl.* **2010**, *12*, E2–E9. [CrossRef]
33. Palomino-Fernández, D.; Seiffert, A.P.; Gómez-Grande, A.; Jiménez López-Guarch, C.; Moreno, G.; Bueno, H.; Gómez, E.J.; Sánchez-González, P. Robustness of [^{18}F]FDG PET/CT Radiomic Analysis in the Setting of Drug-Induced Cardiotoxicity. *Comput. Methods Programs Biomed.* **2024**, *244*, 107981. [CrossRef]

34. Virizuela, J.A.; García, A.M.; de las Peñas, R.; Santaballa, A.; Andrés, R.; Beato, C.; de la Cruz, S.; Gavilá, J.; González-Santiago, S.; Fernández, T.L. SEOM Clinical Guidelines on Cardiovascular Toxicity (2018). *Clin. Transl. Oncol.* **2019**, *21*, 94–105. [CrossRef] [PubMed]
35. Palomino-Fernández, D.; Gómez-Grande, A.; Fernández-Igarza, M.; Pilkington, P.; Seiffert, A.P.; Bueno, H.; Gómez, E.J.; Sánchez-González, P. CASSIA (Cardiology Software Suite for Image Analysis): A Potential New Tool for the Evaluation of [^{18}F]FDG PET/CT in the Setting of Infective Endocarditis. *Int. J. Comput. Assist. Radiol. Surg.* **2023**, *18*, 157–169. [CrossRef] [PubMed]
36. Zwanenburg, A.; Vallières, M.; Abdalah, M.A.; Aerts, H.J.W.L.; Andrearczyk, V.; Apte, A.; Ashrafinia, S.; Bakas, S.; Beukinga, R.J.; Boellaard, R.; et al. The Image Biomarker Standardization Initiative: Standardized Quantitative Radiomics for High-Throughput Image-Based Phenotyping. *Radiology* **2020**, *295*, 328–338. [CrossRef] [PubMed]
37. Manabe, O.; Kroenke, M.; Aikawa, T.; Murayama, A.; Naya, M.; Masuda, A.; Oyama-Manabe, N.; Hirata, K.; Watanabe, S.; Shiga, T.; et al. Volume-Based Glucose Metabolic Analysis of FDG PET/CT: The Optimum Threshold and Conditions to Suppress Physiological Myocardial Uptake. *J. Nucl. Cardiol.* **2019**, *26*, 909–918. [CrossRef]
38. Van Griethuysen, J.J.M.; Fedorov, A.; Parmar, C.; Hosny, A.; Aucoin, N.; Narayan, V.; Beets-Tan, R.G.H.; Fillion-Robin, J.C.; Pieper, S.; Aerts, H.J.W.L. Computational Radiomics System to Decode the Radiographic Phenotype. *Cancer Res.* **2017**, *77*, e104–e107. [CrossRef]
39. Liljequist, D.; Elfving, B.; Roaldsen, K.S. Intraclass Correlation—A Discussion and Demonstration of Basic Features. *PLoS ONE* **2019**, *14*, e0219854. [CrossRef] [PubMed]
40. Koo, T.K.; Li, M.Y. A Guideline of Selecting and Reporting Intraclass Correlation Coefficients for Reliability Research. *J. Chiropr. Med.* **2016**, *15*, 155–163. [CrossRef] [PubMed]
41. Zamorano, J.L.; Lancellotti, P.; Rodriguez Muñoz, D.; Aboyans, V.; Asteggiano, R.; Galderisi, M.; Habib, G.; Lenihan, D.J.; Lip, G.Y.H.; Lyon, A.R.; et al. 2016 ESC Position Paper on Cancer Treatments and Cardiovascular Toxicity Developed under the Auspices of the ESC Committee for Practice Guidelines. *Eur. Heart J.* **2016**, *37*, 2768–2801. [CrossRef]
42. Armenian, S.H.; Lacchetti, C.; Barac, A.; Carver, J.; Constine, L.S.; Denduluri, N.; Dent, S.; Douglas, P.S.; Durand, J.B.; Ewer, M.; et al. Prevention and Monitoring of Cardiac Dysfunction in Survivors of Adult Cancers: American Society of Clinical Oncology Clinical Practice Guideline. *J. Clin. Oncol.* **2017**, *35*, 893–911. [CrossRef] [PubMed]
43. Karlstaedt, A.; Barrett, M.; Hu, R.; Gammons, S.T.; Ky, B. Cardio-Oncology: Understanding the Intersections Between Cardiac Metabolism and Cancer Biology. *JACC Basic Transl. Sci.* **2021**, *6*, 705–718. [CrossRef] [PubMed]
44. Takemura, G.; Fujiwara, H. Doxorubicin-Induced Cardiomyopathy: From the Cardiotoxic Mechanisms to Management. *Prog. Cardiovasc. Dis.* **2007**, *49*, 330–352. [CrossRef] [PubMed]
45. Belger, C.; Abrahams, C.; Imamdin, A.; Lecour, S. Doxorubicin-Induced Cardiotoxicity and Risk Factors. *IJC Heart Vasc.* **2024**, *50*, 101332. [CrossRef] [PubMed]

Disclaimer/Publisher's Note: The statements, opinions and data contained in all publications are solely those of the individual author(s) and contributor(s) and not of MDPI and/or the editor(s). MDPI and/or the editor(s) disclaim responsibility for any injury to people or property resulting from any ideas, methods, instructions or products referred to in the content.